ELSEVIER

PII: S0032-3861(96)00773-2

*Polymer* Vol. 38 No. 9, pp. 2259–2268 1997

0032-3861/97/$17.00 + 0.00

# Solvation of poly(vinyl alcohol) in water, ethanol and an equimolar water–ethanol mixture: structure and dynamics studied by molecular dynamics simulation

**Florian Müller-Plathe* and Wilfred F. van Gunsteren**
*Laboratorium für Physikalische Chemie, Eidgenössische Technische Hochschule Zürich, ETH-Zentrum, CH-8092 Zürich, Switzerland*
*(Received 29 May 1996)*

Solutions of a 15-mer of poly(vinyl alcohol) in water, ethanol and a 1/1 (mole fraction) mixture of water and ethanol have been studied by molecular dynamics simulations. The solvent structure near the solute is analysed in terms of radial distribution functions and hydrogen bonding. Results indicate a preferential solvation by water molecules. Hydrogen-bond life time analysis shows that solvent–solute hydrogen bonds are slightly longer-lived than solvent–solvent hydrogen bonds. However, the separation in time scales is not large enough to support the notion of a solvent-decorated polymer. An analysis of the polymer dynamics shows that the *gauche* ↔ *trans* transitions of backbone dihedral angles are at least an order of magnitude slower than the renewal of intramolecular hydrogen bonds along the polymer chain. No coupling is observed between the two. © 1997 Elsevier Science Ltd.

**(Keywords: poly(vinyl alcohol); membranes; hydrogels)**

## INTRODUCTION

Poly(vinyl alcohol) (PVA; $-(CH_2-CHOH)_n-$) is a polymer which is soluble in water to a large degree but considerably less so in most organic solvents. Many of its applications are determined by its hydrophilicity (researchers have, for example, worried about the water content of PVA films as early as 1946[1]). Among them are the use as hydrogel former and as material for separation membranes where research is still very active[2,3]. It is often used in pervaporation systems for the removal of water (minority component) from liquid mixtures.

In membrane applications, PVA is often cross-linked to prevent dissolution. Such cross-linked networks can swell if brought into contact with a suitable solvent. In pervaporation, the conditions of the membrane are particularly non-uniform: On the feed side, the polymer is immersed into a liquid and, presumably, highly swollen, whereas on the permeate side, it is exposed to a vacuum and, therefore, practically solvent-free. Somewhere between these two extremes is the active layer of the membrane which does the actual separation. Little is understood about the structure of the polymer–solvent system and the processes which give rise to the observed selectivity.

Molecular simulation and, in particular, molecular dynamics (MD) has been successfully applied in membrane science in recent years: Most applications have focused on gas permeation[4–8], and, more recently, polymer electrolytes[4,9–13]. However, a number of simulations have explicitly addressed the swelling of polymer (membranes) in solvents: polystyrene (PS) in benzene[14,15] and poly(dimethyl siloxane) (PDMS) in ethanol[16]. The role of molecular simulation has been two-fold (for reviews, see refs 4 and 5). Firstly, in many cases it allows a quantitative prediction of membrane properties (e.g. the diffusion coefficient of a penetrant in the membrane). Secondly, it can provide microscopic explanations of observed macroscopic phenomena (e.g. the underlying diffusion mechanism), which may then lead to the design of membrane materials with improved properties. Our previous work on PS swollen to various extent by benzene[14,15] has revealed interesting and to some degree counterintuitive features in the solvation of the polymer. One particular result concerned the mobility of solvent molecules: It was shown that solvent molecules near the polymer are as mobile as in the bulk liquid. It was not clear whether this phenomenon is general or whether it is limited to apolar polymers in apolar solvents. A PVA 21-mer in water has recently been studied by MD as part of an investigation into hydrogel-forming polymers[17].

In the present contribution, previous work is extended. Firstly, we study a highly polar polymer in protic solvents. This should help clarify if solvent mobility is uniform also for strongly interacting polymer–solvent systems. Secondly, we study two solvents (water and ethanol) and their mixture in order to find out why and how they differ in their affinity towards PVA. Thirdly, PVA is a membrane material (PS is not) and the removal of water from ethanol is an important industrial application. As a first step, we study a single 15-mer

* To whom correspondence should be addressed. Present address: Max-Planck-Institut für Polymerforschung, D-55128 Mainz, Germany

(pentadecamer) of PVA in three different solutions. Having only one medium-size polymer chain in an excess of solvent suppresses polymer–polymer interactions which could obscure the solvation effects we want to study. At the same time, 15 monomers should be long enough to observe solvent effects on the polymer conformations. It is expected that these can serve as the 'infinite dilution' limit and be taken as a reference point for future investigations with a larger polymer content.

## FORCE FIELD AND SIMULATION DETAILS

Water molecules are treated by the SPC force field[18]. For ethanol, we have recently developed an all-atom force field[19] which not only reproduces known liquid properties of neat ethanol but also of ethanol–water mixtures at all compositions. The PVA force field used here was derived from the ethanol force field by adding bond-angle and dihedral-angle terms not present in ethanol. These were taken from previous simulations of poly(ethylene oxide)[11]. In the ethanol force field, a special third-neighbour interaction had to be introduced between the hydroxyl hydrogen and the methyl carbon to adjust the relative potential energy of *trans* and *gauche* orientations of the hydroxyl group to *ab initio* reference values. Since the energy difference is small, this term has been re-investigated for PVA. To this end, we have performed *ab initio* (HF/6-31G**) and hybrid density functional (B3LYP/6-31G**) calculations of the potential energy curve along the internal rotation of the OH group in 2-propanol (not shown). The dihedral angle defined by the $\alpha$-hydrogen (H1 in the PVA nomenclature of *Figure 1*), the secondary carbon (C1), the oxygen (O) and the hydroxyl hydrogen (H) was held fixed at 30° intervals between 0° and 180°, while all other degrees of freedom were allowed to optimize. Hartree–Fock (HF) gave barriers of 4.5 kJ mol$^{-1}$ (0°) and 5.8 kJ mol$^{-1}$ (±120°) and put the *gauche* conformer (±59.6°) 0.9 kJ mol$^{-1}$ below *trans* (180°). Recall that, in 2-propanol, '*trans*' means *trans* with respect to the $\alpha$-hydrogen but *gauche* with respect to *both* methyl groups, whereas a position *gauche* with respect to the $\alpha$-hydrogen means a *trans* orientation with respect to one methyl group and a *gauche* orientation with respect to the other. B3LYP on the other hand, gave slightly higher barriers (6.5 and 6.2 kJ mol$^{-1}$, respectively) and the *gauche* conformer (±61.8°) 0.5 kJ mol$^{-1}$ above the *trans* conformer. We note that although the two methods give qualitatively different results for the *gauche–trans* equilibrium, both find the energy difference to be at the limit of the accuracy of the methods and also small compared to $k_BT$ at room temperature (2.5 kJ mol$^{-1}$). Since the dipole moments of both conformers are practically identical (1.74 and 1.82 D for *gauche* and *trans*, respectively, at the HF level), going from vacuum to a polarizable solvent will not change matters significantly. We have, therefore, decided not to assume any preferential orientation of the hydroxyl group in PVA, and we have omitted the extra third-neighbour term from the PVA force field.

Three details of the microstructure of PVA are relevant for setting up the simulation. We have to specify the absolute configuration of all monomers. It seems to be the general view that commercial PVA is atactic. We have contacted two suppliers of PVA and have been informed that although they do not have precise information on the tacticity of their polymer they assume it is atactic, because the parent poly(vinyl acetate) was obtained by free radical polymerization. There have been attempts to determine the tacticity of PVA but the results seem to depend on the details of the measurement almost as much as on the sample[20]. We therefore have assumed our 15-mer to be atactic and have randomly assigned monomer configurations. The configuration, denoted as R or L, is defined in the following way: Imagine that the chain is stretched out, i.e. all C–C–C–C dihedrals are *trans*. Then orient the chain such that all C2 point down and all C1 point up (cf. *Figure 1*). If, viewing along the chain from the first to the last monomer, an oxygen points to the right, the configuration is denoted R, otherwise L. In this notation, the absolute configuration of the 15-mer is LLLLR LRLLR RRRRL. The second point concerns the

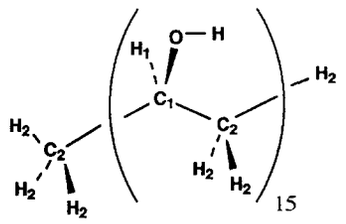


**Figure 1** Atom labelling in the poly(vinyl alcohol) 15-mer

**Table 1** Parameters for the force field for poly(vinyl alcohol). For atom labelling, see *Figure 1*

| Nonbonded interactions[a] | $E_{pot}(r_{ij}) = 4\epsilon_{ij}\left[\left(\frac{\sigma_{ij}}{r_{ij}}\right)^{12} - \left(\frac{\sigma_{ij}}{r_{ij}}\right)^{6}\right] + \frac{q_i q_j}{4\pi\epsilon_0}\left(\frac{1}{r_{ij}} - \frac{r_{RF}-1}{2r_{RF}+1}\frac{r_{ij}^2}{r_{cutoff}^3}\right)$ | | | |
|---|---|---|---|---|
| Atoms | $m$/a.m.u.[b] | $\epsilon$/kJ mol$^{-1}$ [c] | $\sigma$/nm [c] | $q$/e |
| H (OH) | 1.00787 | 0 | 0 | 0.4 |
| O | 15.9949 | 0.65 | 0.317 | −0.7 |
| C1 | 12 | 0.336 | 0.35 | 0.3 |
| C2 | 12 | 0.336 | 0.35 | 0 |
| H1, H2 | 1.00787 | 0.21 | 0.257 | 0 |

| Bond constraints | Length/nm |
|---|---|
| H–O | 0.097 |
| C–O | 0.1431 |
| C–C | 0.153 |
| C–H | 0.11 |

| Bond angles | $E_{pot}(\phi) = \frac{k_\phi}{2}(\varphi - \varphi_0)^2$ | |
|---|---|---|
| | $\varphi_0$/degrees | $k_\phi$/kJ mol$^{-1}$ rad$^{-2}$ |
| H O C | 105 | 320 |
| C–C–C | 109.45 | 482.3 |
| O–C–C | 107.8 | 460 |
| O–C–H | 108 | 350 |
| C–C–H | 110 | 367 |
| H–C–H | 108 | 306 |

| Dihedral angles | $E_{pot}(\tau) = \frac{k_\tau}{2}[1 - \cos 3(\tau - \tau_0)]$ | |
|---|---|---|
| | $\tau_0$/degrees[d] | $k_\tau$/kJ mol$^{-1}$ |
| H–O–C–C | 180 | 6 |
| C–C–C–C | 180 | 11.5 |
| C–C–C–H | 180 | 11.5 |

[a] There are no nonbonded interactions between atoms separated by one or two bonds (first and second neighbours)
[b] Atomic masses are those of the most abundant isotopes
[c] The Lorentz–Berthelot combination rules are used for mixed interactions: $\epsilon_{ij} = (\epsilon_{ii}\epsilon_{jj})^{1/2}$, $\sigma_{ij} = (\sigma_{ii} + \sigma_{jj})/2$
[d] The *cis* conformation corresponds to $\tau = 0°$

**Table 2** Calculated properties of different solutions of the poly(vinyl alcohol) 15-mer at 300 K and 1 atm[a]

| Solvent | $t$ (ns) | $\rho$ (kg m$^{-3}$) | $c_{PVA}$ (kg m$^{-3}$) | $D_{H_2O}$ ($10^{-6}$ cm$^2$ s$^{-1}$) | $D_{EtOH}$ ($10^{-6}$ cm$^2$ s$^{-1}$) | $D_{PVA}$ ($10^{-6}$ cm$^2$ s$^{-1}$) | $\epsilon_r$ |
|---|---|---|---|---|---|---|---|
| 432 $H_2O$ | 2.040 | 989 | 79.1 | 29 | | 2.4 | 102.1 |
| | | (2.7) | | (3.7) | | (0.3) | (14.8) |
| 648 $H_2O$ | 3.748 | 984 | 54.4 | 37 | | 2.6 | 100.7 |
| | | (2.5) | | (2.1) | | (0.9) | (3.7) |
| 162 $H_2O$/162 EtOH | 2.834 | 857 | 52.4 | 10 | 7.1 | 0.75 | 39.5 |
| | | (3.2) | | (0.7) | (1.1) | (0.34) | (2.0) |
| 216 EtOH | 2.768 | 809 | 51.5 | | 6.5 | 0.81 | 27.4 |
| | | (3.1) | | | (0.8) | (0.50) | (1.8) |

[a] $t$, simulated time; $\rho$, mass density of the solution, fluctuations in parentheses; $c_{PVA}$, mass concentration of poly(vinyl alcohol), fluctuations in parentheses; $D_{H_2O}$, $D_{EtOH}$, $D_{PVA}$, tracer diffusion coefficients of water, ethanol and the PVA 15-mer, respectively (in parentheses: standard deviation of the Cartesian components); $\epsilon_r$, relative permittivity (dielectric constant), in parentheses standard deviations of values calculated from fluctuations of individual Cartesian components of the total dipole moment

presence of head-to-head junctions of the polymer, leading to a number of 1,2-diol motifs in addition to the usual 1,3-diol motifs. Head-to-head junctions can reach a few percent in some PVAs[20]. However, in the present work, we assume head-to-tail junctions only. The third choice has to be made with regard to the end groups of the chain. We have chosen to make both ends equivalent and to terminate them on the C2 carbon, both terminal carbons being appropriately saturated by hydrogens (cf. *Figure 1*).

The conformation of the PVA backbone can be specified using all C–C–C–C dihedral angles. In order to generate a starting structure, we have assigned values to these dihedrals randomly drawn from the dihedral angle distribution at 300 K and using the parameters of *Table 1*. Unless noted otherwise, we have allowed the radius of gyration to relax, before any sampling of conformational properties. The PVA chain was then solvated by 648 water molecules, 216 ethanol molecules or 162 molecules of both kinds, corresponding to PVA concentrations of 54.0, 51.5 and 52.4 g l$^{-1}$, respectively. Initially, we also carried out a simulation of PVA in 432 water molecules (79.1 g l$^{-1}$).

Molecular dynamics calculations were carried out with the YASP program[21]. The time step was 2 fs. Temperature $T$ and pressure $p$ were kept constant at 300 K and 101.3 kPa, respectively, by the weak-coupling scheme[22], the coupling times were 0.1 ps ($T$) and 2.0 ps ($p$). All bond lengths were kept rigid by the SHAKE procedure[23]. An atomic neighbour list was used which was updated every 15 time steps and which included all pairs within 1.1 nm. The cut-off for nonbonded interactions was 1.0 nm with a reaction field correction[21]. The choice of the effective dielectric constant (relative permittivity) $\epsilon_{RF}$ used in the reaction-field treatment is not very crucial, once it is above, say, 10. We used 80 for water, 24.3 for ethanol, and 39 for the 1/1 mixture. Simulation times of the various systems are given in *Table 2*.

## RESULTS

### *Solution properties*

We have calculated tracer diffusion coefficients $D$ for all species in the simulations from the slope of the time-dependent centre-of-mass mean-square fluctuations of the molecules (see, e.g. ref. 4). Calculating diffusion coefficients from the mean-square fluctuation is generally more precise than from the mean-square displacement, which is in the present work particularly important for the $D$ of PVA, since the combination of a small diffusion coefficient and poor statistics (only 1 molecule) makes it difficult to be calculated accurately. The $D$ are given in *Table 2*. The $D$ of the solvent molecules are close to those of the pure solvents[19]. The deviation can be accounted for by the simple Mackie–Meares model[24]

$$D/D_0 = (1 - \Phi)^2/(1 + \Phi)^2 \qquad (1)$$

where $D$ is the solvent diffusion coefficient with the polymer present, $D_0$ is the diffusion coefficient of pure solvent under otherwise identical conditions, and $\Phi$ is the polymer volume fraction. We have previously calculated tracer diffusion coefficients of water and ethanol at a slightly lower temperature (20°C)[19]. From published experimental diffusion coefficients[25] it can be estimated that the ratio $D(300\,K)/D(293\,K)$ should be around 1.13 for water and 1.17 for ethanol. If we assume these ratios to hold also for our liquid models, the $D_0$ of water and ethanol at 300 K are estimated to be 38 and $7.5 \times 10^{-6}$ cm$^2$ s$^{-1}$, respectively. The polymer volume fraction $\Phi$, on the other hand, is estimated as the PVA mass concentration $c_{PVA}$ (*Table 2*) divided by the density of amorphous PVA (1260 kg m$^{-3}$ [26]). With these assumptions, equation (1) predicts tracer diffusion coefficients of 29.6, 32.0 and $6.4 \times 10^{-6}$ cm$^2$ s$^{-1}$ for the 432 water, 648 water and 216 ethanol system, respectively, which is reasonably close to the values calculated by MD (*Table 2*). The agreement is better for those systems which are comparable in size to those used to calculate the $D$ of the neat solvents[19]. These findings indicate that the Mackie–Meares approximation (1) seems to hold for PVA/solvent systems with low polymer content. This is not only in agreement with experiment[2], but has also been verified computationally in our work for the polystyrene/benzene system[14,15].

The PVA 15-mer diffuses more slowly than the solvent molecules. This is to be expected because of its size. Its diffusion coefficients are 14 and 8 times smaller than those of the surrounding water and ethanol respectively. This is in line with expectations from the relative sizes of the diffusants. The Stokes–Einstein relation[27] predicts an inverse proportionality of a molecule's diffusion coefficient to its radius under otherwise identical conditions. The radii of gyration of water and ethanol are 0.072 and 0.15 nm, respectively, the average radius of gyration of the PVA 15-mer is about 0.9 nm with large fluctuations (see below). Taking the radii of gyration as measures of

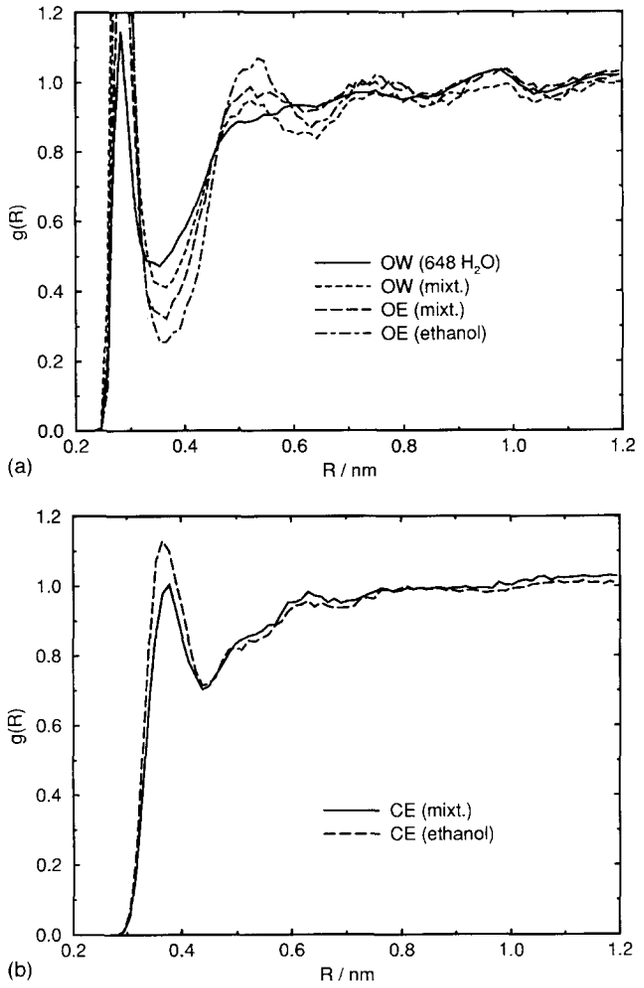


**Figure 2** Solvation of the oxygen atoms of poly(vinyl alcohol). Partial radial distribution functions of PVA oxygen with solvent oxygen (a) and solvent carbon atoms (b). Legend: OW water oxygen, OE ethanol oxygen, CE ethanol carbon

the relative radii of the molecules, Stokes–Einstein predicts diffusion coefficient ratios of 13 for water/PVA and 6 for ethanol/PVA.

The relative permittivity of the solutions (dielectric constant) $\varepsilon_r$ was calculated from the fluctuations of the dipole moment of the total system **M**

$$(\varepsilon_r - 1)\left(\frac{2\varepsilon_{RF} + 1}{2\varepsilon_{RF} + \varepsilon_r}\right) = \frac{\langle M^2\rangle - \langle M\rangle^2}{3\varepsilon_0 V k_B T} \qquad (2)$$

where $V$ is the volume of the simulation cell, $\epsilon_{RF}$ is the relative permittivity used in the reaction field treatment (see above) and $\varepsilon_0$ is the vacuum permittivity. The calculated dielectric constants (*Table 2*) for the PVA solutions are essentially those of the corresponding solvent models[19] indicating that a small polymer content does not significantly alter the part of the solvent dynamics (probably reorientation) which dominates the dielectric response.

*Solvation of poly(vinyl alcohol)*

An average picture of the immediate environment of PVA can be obtained from the partial radial distribution functions (RDF) $g_{AB}(R)$ which describes how many atoms of type $A$ are on average at a distance $R$ of an atom of type $B$[28]. Let $A$ be an atom type of a solvent and $B$ an atom type of PVA. Many pairs of $AB$ combinations are possible. We confine the discussion to $B = O$ (hydrophilic part of PVA) and $B = C = \{C1, C2\}$ (hydrophobic part of PVA) and to the heavy solvent atoms $A = OW$ (water oxygen), $A = OE$ (ethanol oxygen) and $A = CE$ (any ethanol carbon). *Figure 2* describes the situation around the PVA oxygen ($B = O$). In all solvents (*Figure 2a*), the first peak in the RDF is at around 0.3 nm indicating hydrogen bonding of the first solvation shell to a solvent oxygen atom. The $A = OW$, $B = O$ RDF (*Figure 2a*) is very similar to the one of Tamai *et al.*[17] at 300 K, the remaining differences can be explained by a different force field (SPC/E for water and united-atom AMBER/OPLS for PVA). The RDF can be integrated and normalised appropriately to give the number $n_{AB}(R)$ of atoms $A$ in a sphere of radius $R$ around atom $B$

$$n_{AB}(R) = \frac{N_A}{V}\int_0^R 4\pi R'^2 g_{AB}(R')\mathrm{d}R' \qquad (3)$$

where $N_A$ is the number of atoms of type $A$ in the system. Integrating over the first peak in *Figure 2a* to $R =$ 0.35 nm shows that a PVA oxygen has on average 2.5 water oxygens in its first solvation shell if the solvent is pure water, 1.0 OW and 0.7 OE if the solvent contains equal amounts of water and ethanol, and 1.1 OE for pure ethanol as a solvent. This is already a qualitative indication that the hydroxyl groups of PVA are more efficiently solvated by water than by the bulkier ethanol. Tamai *et al.* found a co-ordination of OH by 2.2 water molecules[17] which may be due to the different force field or a slightly different upper integration limit $R$ [equation (3)] for which they do not give a numerical value.

The valley following the first peak is deeper for ethanol than for water and it also deepens with the ethanol content. This is a consequence of the relative molecular size. If an ethanol molecule is hydrogen-bonded to a PVA hydroxyl group, its aliphatic groups will prevent further oxygens (of water or other ethanol molecules) from approaching the PVA causing an area of oxygen depletion at around 0.35 nm. *Figure 2b* shows clearly that this region coincides with the first peak in the O–CE RDF. The second peak of the RDF (*Figure 2a*, 0.5–0.6 nm) shows the same pattern as the minimum between first and second peak. It is more pronounced for OE than for OW and it increases with ethanol content. For pure water, the peak is absent. The reason is that the small water molecules can sit at nearly any distance from the hydroxyl oxygen which smears out this peak, whereas the exclusion of second-shell OE by first-shell CE leads to enrichment of OE immediately beyond the exclusion zone. There is a small third peak in the RDF (*Figure 2a*, 0.65–0.85 nm) for all solvents. The small maximum before 1.0 nm and the small minimum thereafter are residual artefacts of the spherical cut-off at this distance.

The solvation situation around the PVA carbon atoms (both C1 and C2, cf. *Figure 1*) is shown in *Figure 3*. Here, the RDFs with solvent oxygens (*Figure 3a*) show two peaks at short distance ($\approx 0.37$ and $\approx 0.5$ nm) and little solvent structure at larger distances. The two peaks do not arise because of two different environments for C1 and C2 as one might think. Comparing these RDFs separately for $B = C1$ and $B = C2$ (not shown) one finds that the relative heights of these peaks vary, whereas their positions do not. Both PVA carbons are solvated very similarly and both show the two peaks. The first peak arises from a direct contact of a solvent oxygen packed closely to a $CH_1$ or $CH_2$ group, whereas the

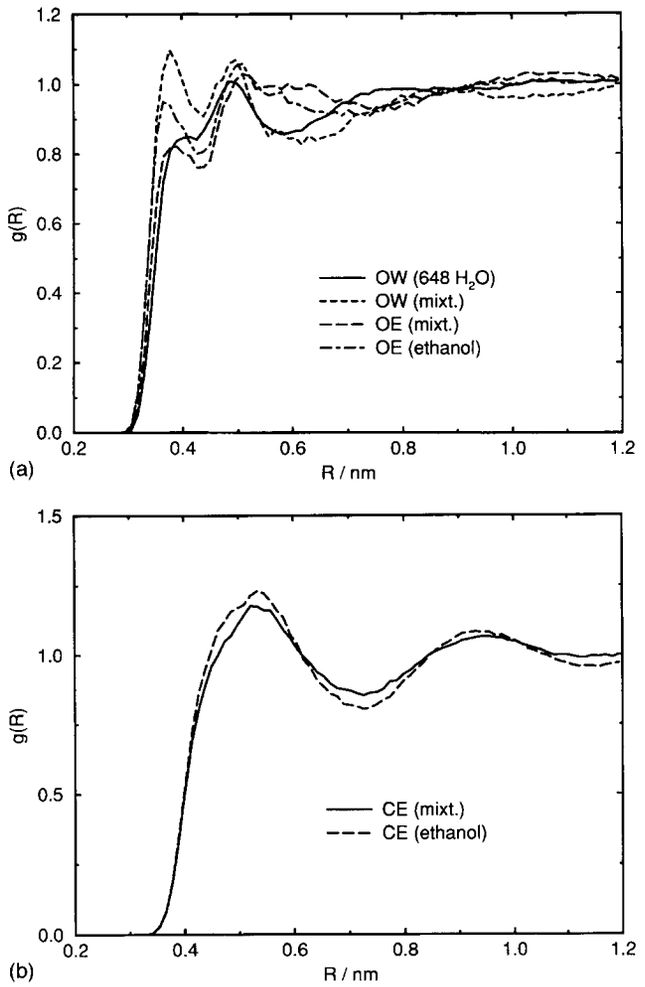


**Figure 3** Solvation of the carbon atoms of poly(vinyl alcohol). Partial radial distribution functions of PVA carbons with solvent oxygen (a) and solvent carbon atoms (b). Legend: OW water oxygen, OE ethanol oxygen, CE ethanol carbon

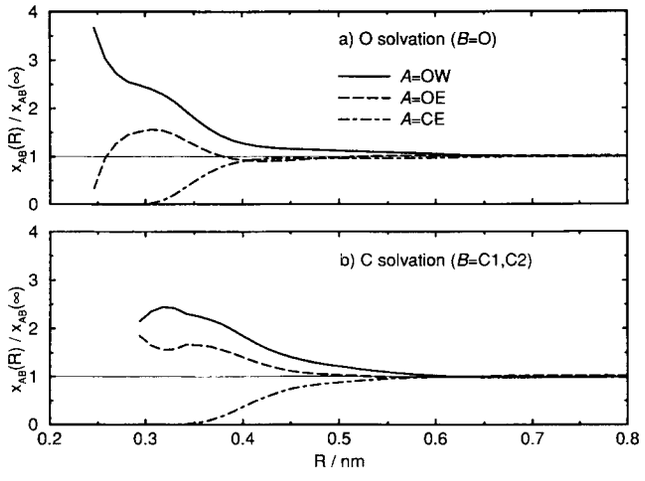


**Figure 4** Solvent competition for poly(vinyl alcohol) oxygen (a) and carbon (b) atoms in the water/ethanol (1:1) mixture: Normalized local atomic fractions. Legend: OW water oxygen, OE ethanol oxygen, CE ethanol carbon

second peak reflects the distance to the solvent oxygen packed against an adjacent $CH_1$ or $CH_2$. One should note, however, that pronounced features in the RDFs at short ranges can be extremely force field dependent[29]. In the RDFs between PVA carbons and ethanol carbons (*Figure 3b*), the short-range double peak is not resolved, since there is now additional averaging over ethanol $C_\alpha$ and $C_\beta$. At 0.45 nm, there is only the hint of a shoulder before the main peak at 0.55 nm.

*Solvent competition and hydrogen bonding*

The competitive solvation of PVA can be studied in the mixed solvent (162 water molecules and 162 ethanol molecules). For the analysis we have used the concept of local molar fractions[30] or, rather, local atomic fractions in the present context. The local atomic fraction $x_{AB}(R)$ of solvent atom type $A$ around a solute atom of type $B$ is defined using the number of neighbours [equation (3)]

$$x_{AB}(R) = \frac{n_{AB}(R)}{\sum_A n_{AB}(R)} \tag{4}$$

where $A$ runs over all non-H solvent atom types (OW, OE, and CE). The local atomic fraction describes the local composition of the solvent in a sphere of radius $R$ around a solute atom $B$. If one normalizes $x_{AB}(R)$ by the corresponding atomic fraction of the bulk solvent, i.e. $x_{AB}(\infty)$, one arrives at a quantity which is 1 if the composition within the radius $R$ is the same as in the bulk, but which is greater (less) than 1 if the solvent sphere contains more (less) of $A$ than the bulk solvent. *Figure 4a* shows the normalized local atomic fractions around PVA oxygens. The preference for water as the closest neighbour is clearly evident. Across the range of the first peak in the RDFs (until 0.35 nm, cf. *Figure 2a*), there is an excess of both OW and OE at the expense of CE. However, there is always more water than ethanol. The OE fraction drops slightly below its bulk value between 0.38 and 0.48 nm due to the exclusion by CE which was already discussed. The excess of OW, on the other hand, persists out to 0.6 nm, possibly due to a secondary shell of water molecules hydrogen-bonded to the first. The solvation of the PVA carbons shows the same global pattern (*Figure 4b*), an excess of OW and OE and a deficiency of CE at short distances which, however, decay smoothly to the bulk values. It is interesting to note that also the environment of PVA carbons is mainly polar. Since there is no strong interaction in the force field between the aliphatic groups of PVA and the polar parts of the solvent, this means that the polar groups of the solvents are attracted by the hydroxyl groups of PVA. The hydrophobic areas of the PVA backbone are probably too small and too close to the hydroxyl groups to show separate hydrophobic solvation (a preferred hydrophobic environment). This confirms the picture of PVA being an entirely hydrophilic polymer.

Another criterion to analyse the solvation of PVA are hydrogen bonds formed by the PVA hydroxyl groups. The importance of hydrogen bonds has already been hinted at in the foregoing discussion of the RDFs. We have analysed the hydrogen bonds formed by the PVA hydroxyl groups. We have adopted a simple geometric criterion: An H-bond is assumed to be present if the distance between the donor and acceptor oxygens is 0.3 nm or less and if the O–H–O angle is 130° or more. These choices are arbitrary to some degree, but the qualitative comparisons reported here are rather insensitive to them.

The hydrogen bonds of a PVA OH group can be classified (i) into internal (intramolecular) or external (to

**Table 3** Hydrogen bonds of the 15 poly(vinyl alcohol) hydroxyl groups. The first line for each system gives the average number of hydrogen bonds of a given type at any time point, the second line gives in parentheses their average lift times (ps)[a]

| Solvent | H → O | H → OW | H → OE | HW → O | HE → O | Ext.[b] | Total[b] |
|---|---|---|---|---|---|---|---|
| 432 $H_2O$ | 4.8 | 5.9 | | 11.7 | | 17.6 | 22.4 |
| | (11.6) | (1.7) | | (2.1) | | | |
| 648 $H_2O$ | 6.1 | 5.0 | | 11.0 | | 16.0 | 22.1 |
| | (13.0) | (1.7) | | (3.3) | | | |
| 162 $H_2O$/162 EtOH | 4.4 | 3.3 | 2.8 | 5.4 | 2.6 | 14.1 | 18.5 |
| | (21.6) | (3.4) | (3.0) | (4.3) | (2.9) | | |
| 216 EtOH | 6.5 | | 5.1 | | 4.6 | 9.7 | 16.2 |
| | (34.4) | | (4.1) | | (3.3) | | |

[a] Atom types (columns headings): H and O denote PVA hydroxyl hydrogen and oxygen, respectively; HW and OW denote water hydrogen and oxygen; HE and OE denote ethanol hydroxyl hydrogen and oxygen. The arrows point from donated hydrogen to acceptor
[b] Ext. and total denote the number of external (to solvent) hydrogen bonds and the total number of hydrogen bonds (intramolecular plus external) of the PVA 15-mer

solvent) and (ii) according to whether the O acts as hydrogen donor or acceptor. This gives rise to the five H-bond types listed in *Table 3*. One notes that there appears to be a systematic decrease in the total number of hydrogen bonds of the PVA 15-mer from 22 in aqueous solution to 16 in ethanol. This is caused by a decrease of the external hydrogen bonds; the number of internal ones (H → O) varies unsystematically (internal hydrogen bonds are discussed below). The smaller number of external hydrogen bonds is caused by the larger space requirement of ethanol as compared to water which prevents further ethanol molecules from approaching the PVA closely, as was already evident from the RDFs (*Figure 2a*). For the solvent mixture, the preference for water as a hydrogen bond partner is evident once more: there are 8.7 hydrogen bonds to water and only 5.4 to ethanol. It is interesting to note that water has a preference for acting as a hydrogen donor rather than an acceptor ((H → OW)/(HW → O) = 5/11). Since one would expect the force field to cause the reverse preference ($q_H \times q_{OW} = -0.4 \times 0.82 < q_{HW} \times q_O = -0.41 \times 0.7$; Lennard–Jones parameters are the same for both combinations, cf. *Table 1*), this has to be explained by geometric reasons. A hydroxyl group can have more incoming (2 approx.) hydrogen bonds but only one outgoing. In particular, if the H is already donated in an intramolecular H bond there can still be two incoming H bonds from water molecules. In the case of ethanol, the effect is much less pronounced and, if anything, the trend is reversed. Here, the size of the ethanol molecules prevents more than one ethanol molecule occupying H donor positions around a PVA hydroxyl.

From *Table 3* one calculates that there are 1.07 external H-bonds per hydroxyl group in water, 0.94 in the mixture, and 0.65 in ethanol. Using quite different geometric criteria for the presence of an H-bond, Tamai *et al.* find 1.8 hydrogen bonds per OH group in water.

*Solvent dynamics*

It is also worth comparing the average life times of hydrogen bonds (*Table 3*). These indicate the relative mobility within the solvation shell. The distribution of life times is in most cases approximately exponential (in contrast to Tamai *et al.*, whose life time distributions look more like stretched exponentials[17]). Hence, it is sufficient to report the average life time. Only the intramolecular hydrogen bonds have a life time distribution which looks more like a stretched exponential. The shortest life times are found for H bonds between PVA and water (≈ 1.8 ps), with a tiny difference between incoming and outgoing H bonds. The life times are about 3.2 ps for the mixed solvent, with a notably longer (4.3 ps) life time for the HW → O bonds. The life times in pure ethanol are longer still (≈ 3.7 ps). This systematic increase of the life times as a function of solvent type is in keeping with the lower solvent mobility as, for instance, reflected by the diffusion coefficients (*Table 2*).

The life times of solute–solvent hydrogen bonds can also be usefully compared to those of solvent–solvent hydrogen bonds. Among the solvent molecules, the average hydrogen bond life times are 1.1 ps (pure water), 2.6 ps (mixture) and 3.2 ps (pure ethanol). In all cases, the life time of the solute–solvent hydrogen bond is longer than that of the average hydrogen bond between two solvent molecules, with the effect strongest for pure water and weakest for pure ethanol. Hence, in the present system whose solute–solvent interaction is dominated by hydrogen bonding we find a difference in local mobility for solvent molecules close to the solute compared to those in the bulk. In a previous study on polystyrene in benzene where the interactions are weaker (dispersion and quadrupole–quadrupole) there was no difference detectable. This leads to the conclusion that with a stronger solute–solvent attraction the difference in mobility increases. However, even in the most pronounced case of water, the effect is small and the mobilities are still of the same order. Therefore, it is probably not justified to conceptually separate the solvent into 'solute-bound' and 'free' molecules.

*Chain extension*

The spatial extension of a polymer chain is often regarded as a result of solvent quality[31]. It can be measured by the radius of gyration or the end-to-end distance (here the distance of the C2 atoms of the two terminal methyl groups) of the polymer. *Figures 5* and *6* show the time development of these two quantities for the PVA 15-mer in three different solvents. The initial chain conformation which is the same random coil for all systems is too compact and the radius of gyration $R_g$ takes several hundred ps to converge to its final value. In *Figure 5*, this is clearly visible for the solvent mixture and pure ethanol. (The final chain conformation of the 432 water solvent was taken as the initial conformation for the 648 water solvent. Hence, for water, there is no equilibration phase visible in *Figure 5*.) The expansion of

the chain in the solvent mixture appears to go through an intermediate step which exists for about a ns before the final expansion takes place. It is not clear if this is a transient feature or if it is part of the equilibrium ensemble of polymer structures. The end-to-end distances converge to their final range much quicker than $R_g$, probably because their relative fluctuations are larger. As a result of that, no plateau similar to that found in the $R_g$ for the solvent mixture is observed for the end-to-end distance. The averages of $R_g$ and the end-to-end distance are rather similar for all solvents (*Table 4*), the largest average being found for the mixture. The ratio of end-to-end distance and $R_g$ already tells that the 15-mer is too short to exhibit polymer chain statistics. For a chain long enough to be considered a random walk it would be equal to $\sqrt{6} \approx 2.4$, whereas from *Table 4* values between 1.4 and 1.9 are calculated.

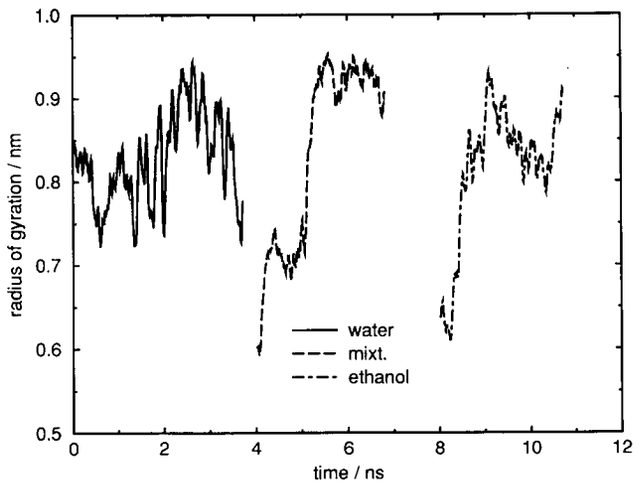


**Figure 5** Time evolution of the radius of gyration of the poly(vinyl alcohol) 15-mer in solution. The water curve is that of the 648-water system. The curves for the water/ethanol mixture and pure ethanol are offset in $x$ direction by 4 and 8 ns, respectively

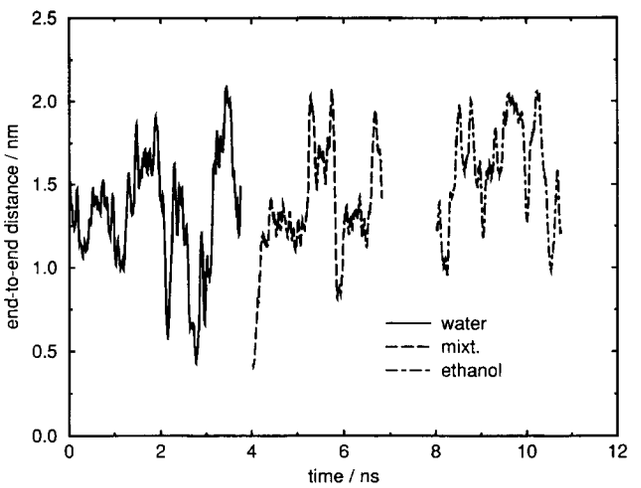


**Figure 6** Time evolution of the end-to-end distance of the poly(vinyl alcohol) 15-mer in solution. The water curve is that of the 648-water system. The curves for the water/ethanol mixture and pure ethanol are offset in $x$ direction by 4 and 8 ns, respectively

*Polymer local conformation*

Intramolecular distances can be analysed in the same way as the end-to-end distance. We have studied the distribution of inter-monomer distances in the PVA 15-mer. As the inter-monomer distance $d(k)$ we take the distance between the C1 carbon atoms of monomers separated by a topological distance $k$; $k = 1$, e.g. denotes nearest neighbours. For $k$ sufficiently large, $d(k)$ depends on $k$ by a power law for many idealized and real polymers

$$\frac{\langle d^2(k)\rangle}{\langle d^2(1)\rangle} = k^n \tag{5}$$

The exponent $n$ would equal 2 for a rigid rod polymer, 1 for an unperturbed polymer chain (theta conditions) and 6/5 for a polymer in a good solvent[31]. In a doubly logarithmic plot of equation (5) for the PVA 15-mer in different solvents, the slope is equal to $n$ (*Figure 7*). For small $k$ (below 7, say), $n$ is about 1.5–1.8, indicating a tendency for the polymer to form linear stretches on the length scale of six monomers. This is observed in all solvents. Between $k = 7$ and $k = 10$, however, the power law changes to a lower $n$. Both the chain length of 15 and the simulation times are too short to establish unambiguously a limiting value of $n$. Similarly, the fluctuations (indicated by error bars for the water curve) are so large for the higher $k$ that no distinction between different solvents is possible. However, it is safe to assume that subunits of at least 10 monomers have to be considered as basic building blocks before one can expect to observe chain statistics typical of a generic polymer.

This view is supported by the distributions of $d(k)$ for the different $k$. These are shown in *Figure 8* for the aqueous solution of PVA. Strong structuring is seen for the distributions with $k = 1$–5, indicating a finite number of distinguishable rotational isomers. At larger $k$, the detailed features are lost and the distribution approaches a Gaussian. The distributions with $k = 10$–14 are indistinguishable within their respective errors and are shown only as an average. The distributions are very similar for the different solvents, as is shown for the small $k$ (2–5) in *Figure 9*. The main peaks occur at the same positions and vary only slightly in relative height. Differences are found mainly at short distances.

*Dihedral angle distribution and isomerization dynamics*

Characteristics of the polymer can also be studied in terms of the dihedral angles defined by the backbone

**Table 4** Extension of the poly(vinyl alcohol) 15-mer in solution. The sampling interval pertains to the calculation of the radius of gyration, the end-to-end distance has been calculated from the entire simulations. Fluctuations are given in parentheses

| Solvent | Sampling interval (ps) | Radius of gyration (nm) | End-to-end distance (nm) |
|---|---|---|---|
| 432 $H_2O$ | 400–2040 | 0.75 (0.04) | 1.37 (0.21) |
| 648 $H_2O$ | 0–3644 | 0.80 (0.04) | 1.31 (0.21) |
| 162 $H_2O$/162 EtOH | 1300–2834 | 0.92 (0.02) | 1.34 (0.35) |
| 216 EtOH | 500–2768 | 0.85 (0.04) | 1.60 (0.32) |

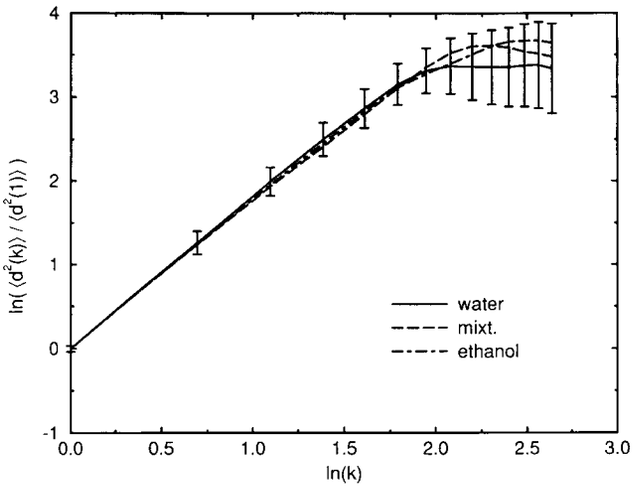


**Figure 7** The average distance $d(k)$ between C1 carbons which are $k$ monomers apart [equation (5)] for the poly(vinyl alcohol) 15-mer in 648 water, the water/ethanol mixture and pure ethanol. Error bars on the water curve indicate the fluctuations, which are very similar for the other solvents

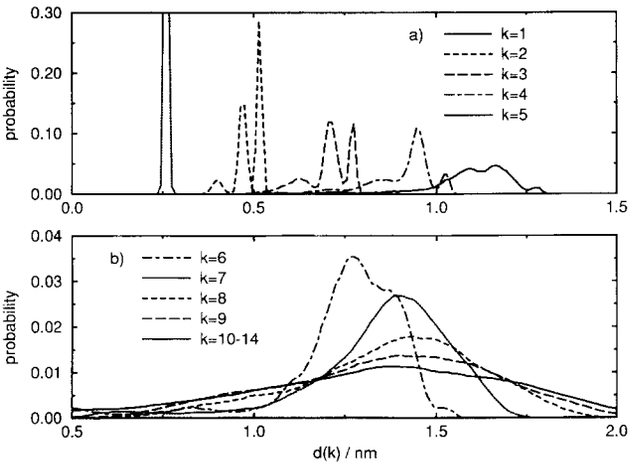


**Figure 8** Distribution of the distances $d(k)$ between C1 carbons which are $k$ monomers apart for the poly(vinyl alcohol) 15-mer in 648 water

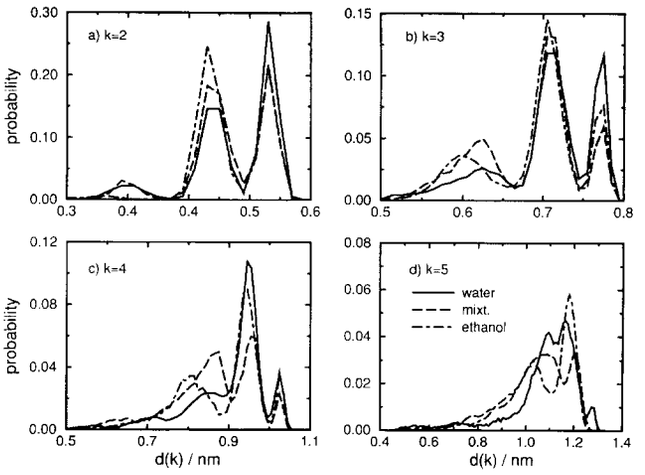


**Figure 9** Comparison of the $d(k)$ distributions for small $k$ in different solvents. For clarity, running averages are shown for some of the curves

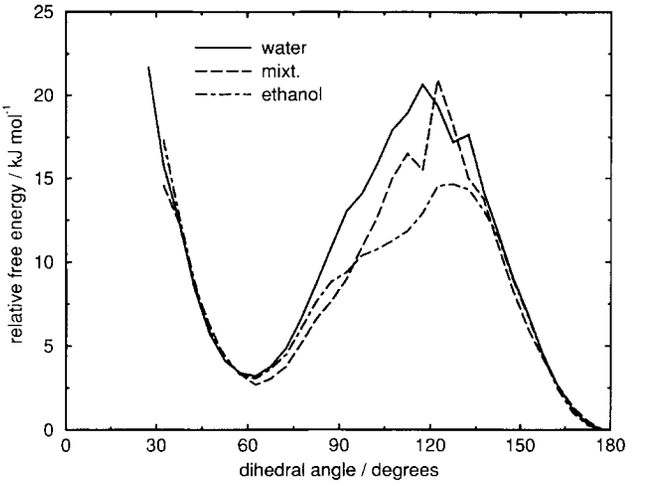


**Figure 10** Relative free energy (potential of mean force) along the backbone dihedral angles (C1–C2–C1–C2) of the poly(vinyl alcohol) 15-mer. The water curve is for 648 water molecules, for the mixture sampling was only performed after the final expansion in the radius of gyration (time > 1.3 ns, cf. *Figure 5*)

carbon atoms. For their distribution reasonable statistics can be obtained because they are all equivalent. The distribution $P(\tau)$ can be converted to a potential of mean force [free energy $A(\tau)$] as a function of the dihedral angle $\tau$

$$-k_B T \ln(P(\tau)/P_0) = A(\tau) - A_0 \qquad (6)$$

where $P_0$ is the largest value of the distribution and $A_0$ is the corresponding minimum of the free energy. This free-energy profile is shown in *Figure 10* for all solvents. In all solvents, the backbone dihedrals are preferentially *trans* (T, 180°). The *gauche* states ($G^+$, $G^-$, ±62°) have free energies approximately 3.2 kJ mol$^{-1}$ above *trans* both for water and ethanol solvents. The lower *gauche* free energy of the mixture (2.6 kJ mol$^{-1}$) is not significantly different. During our simulations the *cis* barrier was never crossed. The most conspicuous difference between the solvents is found for the TG barrier (≈120°). In water and water/ethanol it is about 18–22 kJ mol$^{-1}$ whereas in ethanol it is about 14 kJ mol$^{-1}$.

It would be interesting to investigate in detail the distribution of dyads (two consecutive torsional angles) because of their direct relevance to rotational isomeric state theory. However, much better statistics and, hence, much longer runs would be needed. We can only classify the dyads by the rotational states (T, $G^+$, $G^-$) of the two dihedral angles, and even then the errors are large. The dyad probabilities are, nonetheless, reported in *Table 5*.

**Table 5** Probabilities for the occurrence of combinations of rotational states of two consecutive dihedral angles in the poly(vinyl alcohol) 15-mer in aqueous solution. The probabilities are given for three types of dihedral angle pairs: C1(R) denotes a dyad flanking a C1 atom whose absolute configuration is R, C2(RR) denotes a dyad flanked by two C1 atoms whose absolute configurations are both R, C2(RL) is the same as C2(RR) but with one C1 having R, the other L configuration. The probabilities of other dyads are symmetry-related

| Rotational states[a] | C1(R) | C2(RR) | C2(RL) |
|---|---|---|---|
| $G^-G^-$, $G^+G^+$ | 0.04 | 0.02 | 0.08 |
| $G^-G^+$, $G^+G^-$ | < 0.01 | 0 | 0 |
| $G^-T$ | 0.19 | 0.16 | 0.20 |
| $G^+T$ | 0.03 | 0.05 | 0.05 |
| TG | 0.03 | 0.05 | 0.20 |
| $TG^+$ | 0.19 | 0.16 | 0.05 |
| TT | 0.49 | 0.55 | 0.40 |

[a] T: *trans* (≈180°), $G^+$: *gauche*$^+$ (≈+60°)

for aqueous solutions only, since differences between the solvents are obscured by the inherent errors. For all types of dyads (the bonds under consideration flanking either a C1 or a C2 with different absolute configurations), we find essentially the same qualitative picture. The preferred arrangement is TT with a probability of 0.4–0.5, the second most important is a suitable combination of T and G (0.15–0.2). The other TG combinations have a significantly lower probability as have the $G^+G^+$ and $G^-G^-$ combinations, because here there is an unfavourable 1,5 contact of a carbon and an oxygen separated by three bonds. The $G^+G^-$ and $G^-G^+$ combinations would generate bad 1,5 overlaps of backbone groups and are completely avoided (the well-known 'pentane effect'). With the clear preference for TT dyads, the chain conformational statistics for small numbers of monomers (previous section) becomes understandable.

Monitoring the dihedral angles throughout the simulation allows one to detect transitions between rotational states. The transitions occur between the *trans* state and one of the *gauche* states. A correlation function mechanism has been applied previously[11] that, however, needs many transitions in order to provide reliable results. In this study, we simply count the number of dihedral angle transitions and then calculate the average rate by which the individual dihedral angle changes state. The rates are found to be 0.26, 0.39, 0.74 and 1.68 $ns^{-1}$, for PVA in 432 water, 648 water, water/ethanol, and ethanol, respectively. Hence, we find that the microscopic rearrangement of PVA in ethanol is about 4–5 times faster than in water, which is in keeping with the lower effective barrier (cf. *Figure 10*). We have also examined the contributions of individual dihedrals to the average transition rate (not shown). In all solvents, between 2/3 and 3/4 of the dihedral angles are static, i.e. do not undergo any transition, whereas the remaining dihedral angles show several transitions. The volatile dihedral angles are evenly spread along the polymer, i.e. there is no tendency for dihedrals at the chain ends to show an enhanced transition rate, with the exception of the ethanol solvent where one of the terminal dihedrals seems to be very mobile. However, even discounting this one dihedral, the rate of PVA in ethanol would still be 1.06 $ns^{-1}$, larger than in any other solvent. This means, that in ethanol also the transitions in the inner chain occur more often.

*Hydrogen bonding within the polymer*

It was already noted that the average number of internal hydrogen bonds does not vary greatly between different solvents (*Table 3*). In water, we find on average 0.4 internal H-bonds per OH group which is the same as Tamai *et al.* have found[17] at 300 K. We have classified the internal hydrogen bonds according to the topological distance of the hydroxyl groups in the same way we classified the inter-monomer distances (see above). We find that most hydrogen bonds are between neighbouring OH groups ($k = 1$). The fraction of $k = 1$ H-bonds is 0.95 and 0.97, in pure water and ethanol, but only 0.82 in the solvent mixture. We have found both 'unidirectional' pairs (one OH is always the hydrogen donor, the other always the acceptor) and pairs in which the roles of donor and acceptor change frequently, particularly in aqueous solution. The remaining intramolecular bonds are almost exclusively $k = 2$ bonds, i.e. next-nearest neighbour bonds. There are tiny fractions of $k = 4$ bonds in ethanol and in the mixture, and $k = 11$–$13$ in water. Contacts of intermediate $k$ seem to be unfavourable, which supports the view of PVA being relatively rigid on the length scale of the separation of 7–10 monomers.

The life time of the intramolecular hydrogen bonds changes systematically with the solvent. Going from water to ethanol it increases by a factor of 2.8 from 12 ps to 34 ps (*Table 3*). This is at first puzzling, since the PVA backbone dynamics shows the opposite trend, as exemplified by the dihedral angle transition rates (previous section). One would think, that a $k = 1$ hydrogen bond will have to be broken when a backbone dihedral flips into a new conformation; or, alternatively, the new backbone conformation allows the existence of a hydrogen bond that previously could not be formed. However, it appears that both processes are not coupled. This is understandable, since their time scales are separated by at least an order of magnitude: The longest H-bond life time is 34 ps (in ethanol) and the shortest average residence time of a dihedral angle is 600 ps (also in ethanol). This means that during the average life of a rotational conformation, the average H bond has been formed and destroyed 17 times. We believe that the time scale for internal H bond renewal is much more driven by the time scale with which H bonds between solute and solvent are formed and broken. The ratio of life times for outgoing hydrogen bonds (H → OE to H → OW) is 2.4, for incoming H bonds (HE → O to HW → O), it is 1.7. It seems reasonable that the correlation of the internal H bonds is stronger with that of the outgoing solute–solvent bonds than with the incoming ones. There is a direct competition for a hydroxyl H by two acceptors, the neighbouring OH group or a solvent oxygen. The more often solvent oxygen is offered as an acceptor, the more often an intramolecular H bond will be broken. On the other hand, the competition is not as severe with incoming H bonds, since an intramolecular bond may exist, while both involved hydroxyl groups accept incoming H bonds from solvent and exchange them.

## SUMMARY

From our simulations, poly(vinyl alcohol) appears to be entirely hydrophilic polymer. The comparison between solutions in water and in ethanol shows a clear preference for an aqueous environment, even though water and ethanol are not all that different. We believe that the key is the smaller size of water molecules that allows the OH groups of PVA to simultaneously form more hydrogen bonds to water than to ethanol. This view is supported by the importance of incoming hydrogen bonds (O acting as the H acceptor) for water. In the hydrogen bonding pattern of PVA and ethanol, on the other hand, an equal number of hydrogen bonds goes in both directions. In the case of a 1/1 solvent mixture where direct competition of the two solvents for places near the PVA hydroxyl groups is possible, the analysis of the local atomic fractions shows an excess of water in the first solvent shell. The solvation of the hydroxyl groups also determines the neighbourhood of the PVA methylene and methine groups. The distance between OH groups is not large enough to allow these apolar groups to develop a separate hydrophobic solvation structure.

The mobility of solvent was studied in several ways. The solvent diffusion coefficient is decreased by the presence of polymer. The magnitude of the decrease is

consistent with a model which regards the polymer as a geometric obstacle to diffusion. The solvent reorientation has been studied only indirectly by the dielectric constant, which shows little effect from the presence of polymer. This is in marked contrast to previous simulations with higher polymer content[14,15], where the characteristics of solvent reorientation were changed completely by the polymer. The study of lifetimes of hydrogen bonds between solvent and solute reveals that the mobility of solvent molecules close to the polymer is lowered with respect to the bulk. This effect is larger than previously found in benzene/polystyrene systems[14,15] which we attribute to the stronger solute–solvent interactions (hydrogen bond vs. quadrupole–quadrupole and dispersion). However, it is still too small to justify the concept of a 'solvent-decorated' polymer.

The pentadecamer of PVA studied here is clearly too short to study the long-range chain statistics of PVA in different solvents. The distributions of the inter-monomer distances show strong features up to topological distances of 7 or so. These arise from excluded volume, a finite number of allowed rotational states as well as effective potential of mean force due to the solvent. We estimate that, in order to study directly the chain extension as a function of solvent, one would need chains of a minimum of 50 monomers, which, however, cannot be expected to relax to equilibrium during currently feasible molecular dynamics time scales of a few ns. An alternative route might be more promising: Conversion of the distributions of inter-monomer distances into a potential of mean force to be used in a coarse-grained model of PVA in solution. Nevertheless, the local structure of PVA can be analysed. We find that the preferred conformation of backbone dihedral angles is *trans* with the *gauche* state only about $3\,kJ\,mol^{-1}$ higher in free energy. Dyads are predominately *trans–trans* with the second fraction being two of the possible *trans–gauche* combinations.

Both the potentials of mean force for backbone dihedral angles and the observed rotational isomerization rates indicate that the backbone of PVA is more flexible in ethanol than in water. The life times of intramolecular hydrogen bonds within PVA show the opposite trend, their renewal being slower in ethanol than in water. Since the characteristic time scales for both processes are separated by at least an order of magnitude, we believe that they are not coupled. There is evidence that the renewal of internal hydrogen bonds is largely determined by the dynamics of solute–solvent hydrogen bonding.

## REFERENCES


1 Creutz, E. and Wilson, R. R. *J. Chem. Phys.* 1946, **14,** 725
2 Uchytil, P., Nguyen, Q. T., Clément, R., Grosse, J. M. and Essamri, A. *Polymer* 1996, **37,** 93
3 Petit, J.-M., Zhu, X. X. and Macdonald, P. M. *Macromolecules* 1996, **29,** 70
4 Müller-Plathe, F. *Acta Polym.* 1994, **45,** 259
5 Gusev, A. A., Müller-Plathe, F., van Gunsteren, W. F. and Suter, U. W. *Adv. Polym. Sci.* 1994, **116,** 207
6 Müller-Plathe, F. *J. Chem. Phys.* 1995, **103,** 4346
7 Tamai, Y., Tanaka, H. and Nakanishi, K. *Macromolecules* 1994, **27,** 4498
8 Hofmann, D., Ulbrich, J., Fritsch, D. and Paul, D. *Polymer* (in press)
9 Mills, G. E. and Catlow, C. R. A. *J. Chem. Soc., Chem. Commun.* 1994, **18,** 2037
10 Neyertz, S., Thomas, J. O. and Brown, D. *Comp. Polym. Sci.* 1995, **5,** 107
11 Müller-Plathe, F. and van Gunsteren, W. F. *J. Chem. Phys.* 1995, **103,** 4745
12 Müller-Plathe, F., Liu, H. and van Gunsteren, W. F. *Comp. Polym. Sci.* 1995, **5,** 89
13 Laasonen, K. and Klein, M. L. *J. Chem. Soc., Faraday Trans.* 1995, **91,** 2633
14 Müller-Plathe, F. *Chem. Phys. Lett.* 1996, **252,** 419
15 Müller-Plathe, F. *Macromolecules* 1996, **29,** 4782
16 Fritz, L. and Hofmann, D. *Polymer* (in press)
17 Tamai, Y., Tanaka, H. and Nakanishi, K. *Mol. Sim.* 1996, **16,** 359
18 Berendsen, H. J. C., Postma, J. P. M., van Gunsteren, W. F. and Hermans, J. in 'Intermolecular Forces' (Ed. B. Pullman), Reidel, Dordrecht, 1981, pp. 331–342
19 Müller-Plathe, F. *Mol. Sim.* (in press)
20 Pritchard, J. G. 'Poly(vinyl alcohol). Basic Properties and Uses', Gordon and Breach, London, 1970
21 Müller-Plathe, F. *Comput. Phys. Commun.* 1993, **78,** 77
22 Berendsen, H. J. C., Postma, J. P. M., van Gunsteren, W. F., Di Nola, A. and Haak, J. R. *J. Chem. Phys.* 1984, **81,** 3684
23 Ryckaert, J.-P., Ciccotti, G. and Berendsen, H. J. C. *J. Comp. Phys.* 1977, **23,** 327
24 Mackie, J. S. and Meares, P. *Proc. R. Soc. Lond.* 1955, **A232,** 498
25 'Landolt–Börnstein', various volumes and years, Springer, Heidelberg
26 Davidson, R. L. (Ed.) 'Handbook of Water-Soluble Gums and Resins', McGraw-Hill, New York, 1980
27 Atkins, P. W. 'Physical Chemistry', 5th Edn, Oxford University Press, Oxford, 1994
28 Allen, M. P. and Tildesley, D. J. 'Computer Simulation of Liquids', Oxford University Press, Oxford, 1987
29 Liu, H., Müller-Plathe, F. and van Gunsteren, W. F. *J. Am. Chem. Soc.* 1995, **117,** 4363
30 Scott, W. R. P., Müller-Plathe, F. and van Gunsteren, W. F. *Mol. Phys.* 1994, **82,** 1049
31 Gedde, U. W. 'Polymer Physics', Chapman & Hall, London, 1995